Taming the Lewis Superacid Al(OR F)3 (R F =C(CF3)3): DFT Guided Identification of the "Stable yet Reactive" Adduct S i Pr2→Al(OR F)3; Its Use as OR F-Abstractor from a "Ni-OR F " complex

Julien Petit, Julien Babinot, Nathalie Saffon-Merceron, Lionel Magna, Nicolas Mézailles

Taming the Lewis Superacid $Al(OR^F)_3$ (R^F=$C(CF_3)_3$): DFT Guided Identification of the "Stable yet Reactive" Adduct $S^iPr_2 \rightarrow Al(OR^F)_3$; Its Use as OR^{F-} Abstractor from a "Ni-OR^F" complex.

Julien Petit,[a,b] Julien Babinot,[a] Nathalie Saffon-Merceron,[c] Lionel Magna,*[b] Nicolas Mézailles.*[a]

[a] Dr. J. Petit, Dr. J. Babinot, Dr. N. Mézailles
Université Paul Sabatier
Laboratoire Hétérochimie Fondamentale et Appliquée
UMR 5069, 31062, Toulouse, France
nicolas.mezailles1@univ-tlse3.fr
[b] Dr. J. Petit, Dr. L. Magna
IFP Energies Nouvelles
Rond-point de l'échangeur, BP3, 69360, Solaize, France
lionel.magna@ifpen.fr
[c] Dr. N. Saffon-Merceron
Université Paul Sabatier
Institut de Chimie de Toulouse
ICT – FR2599, 31062, Toulouse, France

Abstract: A DFT study of several $L \rightarrow Al(OR^F)_3$ (L = Lewis bases) adducts allowed the identification of $(^iPr_2S) \rightarrow Al(OR^F)_3$ **1-S^{i}Pr$_2$** as a "stable yet reactive" adduct. **1-S^{i}Pr$_2$** was shown to act as a masked Lewis superacid able to release $Al(OR^F)_3$ under mild conditions. It could be used to abstract a OR^{F-} ligand from $(bipyMe_2)Ni(OR^F)_2$ (bipyMe$_2$: 6,6'-dimethyl-2,2'-dipyridyl) and generate the nickel alkoxide complex $[(bipyMe_2)Ni(OR^F)(^iPr_2S)]^+[(R^FO)_3Al\text{-}F\text{-}Al(OR^F)_3]^-$ **5**. Ligand exchange of $^iPr_2S$ by Ph_3P yielded $[(bipyMe_2)Ni(OR^F)(PPh_3)]^+[(R^FO)_3Al\text{-}F\text{-}Al(OR^F)_3]^-$ **6**.

Introduction

A very general method to allow substrate coordination at a given metal center is to create a temporarily vacant coordination site via halide abstraction. In numerous cases it can be achieved using salts featuring weakly coordinating anion (WCA). When the halogen metathesis is favorable, Li^+[1,2] or Na^+[3,4] salts are recommended. In more challenging cases, silver salts[5,6] (or thallium salts when redox processes occur with Ag^+),[7,8] are to be employed to precipitate the corresponding metal halide (Scheme 1, top). Krossing et al. have reported in the past years very elegant studies dedicated to the isolation of reactive cationic metal complexes using various salts of the aluminate $[Al(OR^F)_4]^-$ (R^F=$C(CF_3)_3$).[9–13] Many other WCA derivatives salts allowed the access to reactive cationic species as well.[14–16]

We wondered about an alternative strategy that would avoid the use of potentially oxidizing Ag^+ or toxic Tl^+. In order to obtain similar complexes, featuring aluminate $[Al(OR^F)_3(OR)]^-$ or $[Al(OR^F)_4]^-$ counter anions, two conditions are to be met: a) a general access to M-OR or M-OR^F complexes and b) the use of an appropriate base-stabilized strong Lewis acid $Al(OR^F)_3$ (Scheme 1, bottom).

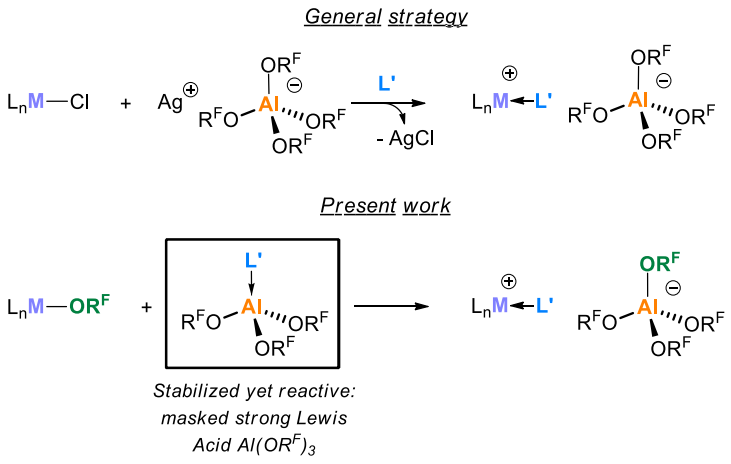

Scheme 1 – Comparative methods to access cationic complexes (R^F=$C(CF_3)_3$).

Metal-alkoxides are well established and understood for early transition metals (group 4 to 6).[17,18].The additional donation of electron density from the oxygen lone pairs to the empty d orbitals result in multiple bond character to the M-O bond, and therefore increased stability (M : early transition metals, Scheme 2 left). On the other hand, examples of M-O bond, with M being a late transition metal, remain scarce.[19,20] Indeed, in these cases, the d_{XY} orbital of d_8-d_{10} metals is occupied, leading to a repulsive interaction with the electron pairs of oxygen (Scheme 2, right).[21] Due to this disfavored interaction, such M-OR bonds are reported to be as reactive as M-C bonds.[22] Notably, a requisite for the stability of M-OR bonds is the lack of β-H that would favor M-H and carbonyl derivative formation via β-H elimination.[23] Focusing on Ni, the use of bulky alkoxide ligands,[23–32] of tridentate ligands,[25,33–39] or the formation of dimer[40] have allowed isolation of stable complexes.

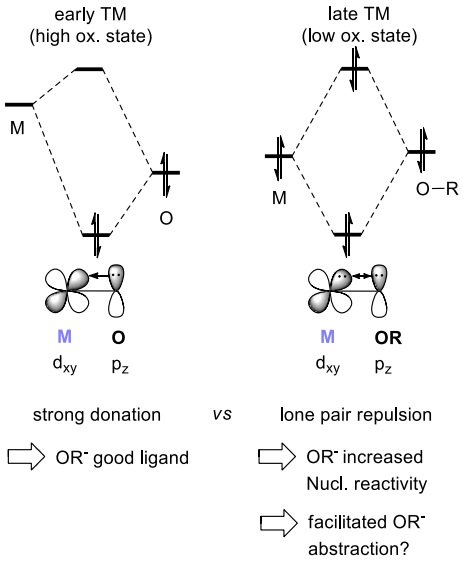

Scheme 2 – Schematic metal oxygen interactions. Early TM = d_4-d_6 metals. Late TM = d_8-d_{10} metals.

Apart from these scattered examples, complexes featuring Ni-O bonds are quite reactive. For example nickel-alkoxides are demonstrated to be intermediates in coupling processes (via ligand exchange or β-H abstraction, Scheme 3, top).[23,41–46] Furthermore, insertion in Ni-O bonds of CO_2, CO, nitriles, ketones, isocyanate (Scheme 3, bottom);[35,36,38,39] has been established for neutral mono-alkoxide nickel complexes; as well as $[OR]^-$ ligand exchange [33] and formal reductive elimination at Ni[37].

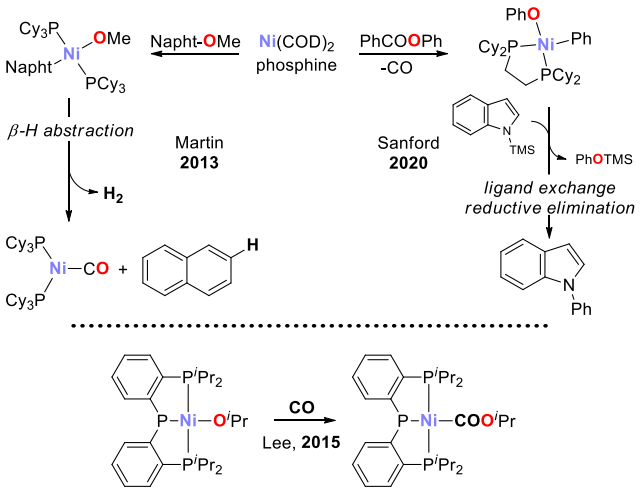

Scheme 3 – Top: Ni-O bonds as intermediates in cross-couplings reactions.[23,46] Bottom: one example of insertion in a Ni-O bond.[37]

During these studies, and as mentioned by Krossing et al., we observed that PhF→Al(OR^F)$_3$ adduct suffers from poor thermal stability liberating the Al(OR^F)$_3$ Lewis acid at room temperature, that evolves via abstraction of one of its own fluorine to form the [(R^{F}O)$_2$Al(μ-F)]$_3$ ring **2** (see below, Scheme 4).[47] We thus felt that it would be desirable to develop novel L→Al(OR^F)$_3$ adducts, that would possess increased stability compared to PhF→Al(OR^F)$_3$ to allow convenient preparation and storage, yet that would generate Al(OR^F)$_3$ under mild conditions. We wish here to present a DFT guided approach to the synthesis of such L→Al(OR^F)$_3$ adducts, based on the strength of the L→Al interaction. Syntheses of two such examples are given, and their stability evaluated. We also show that our new L→Al(OR^F)$_3$ adduct allows for the isolation of monomeric cationic nickel-alkoxide complex [(bipyMe$_2$)Ni(L)(OR^F)]$^+$ from the (bipyMe$_2$)Ni(OR^F)$_2$ complex **3** under mild conditions (Scheme 4, bipyMe$_2$: 6,6'-dimethyl-2,2'-dipyridyl). DFT calculations rationalizing the mechanism of this transformation are presented. Finally, a comparison with the classical abstraction of chloride ligand of the (bipyMe$_2$)NiCl$_2$ analogue revealed a marked difference highlighting the potential of this novel strategy.

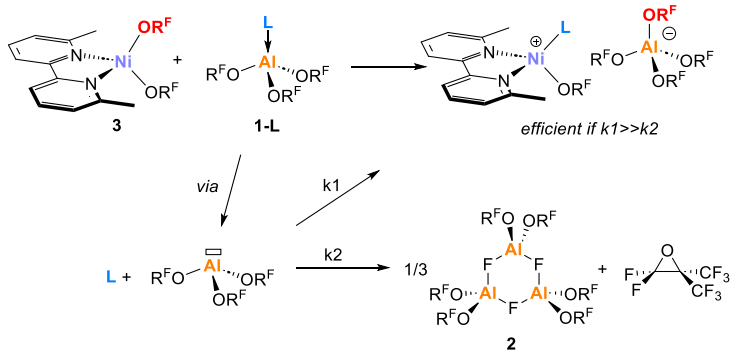

Scheme 4 – Study of the reactivity between (bipyMe$_2$)Ni(OR^F)$_2$ and a newly designed L→Al(OR^F)$_3$ Lewis adduct and isolation of a cationic nickel alkoxide complex. bipyMe$_2$ = 6,6'-dimethyl-2,2'-dipyridyl. R^F = C(CF$_3$)$_3$.

Results and Discussion

DFT guided synthetic targets. To embark in the DFT guided study of desirable "isolable yet reactive" L→Al(OR^F)$_3$ derivatives, the [OR^F]$^-$ abstraction in (bipyMe$_2$)Ni(OR^F)$_2$ **3** by two known L→Al(OR^F)$_3$ (L = C$_6$H$_5$F = PhF, **1-PhF** ; L=Et$_2$O, **1-Et$_2$O**) was used as benchmark reaction. The efficiency of this reaction depends on a) L→Al bond dissociation, directly linked to the bond strength b) the kinetics of Al(OR^F)$_3$ decomposition and c) kinetics of [OR^F]$^-$ abstraction (Scheme 4).

The Et$_2$O→Al(OR^F)$_3$ adduct **1-Et$_2$O** is reported to be stable at room temperature.[48] Not surprisingly, no reactivity was observed between the adduct **1-Et$_2$O** and complex **3**, even at 80°C for 24h, which was attributed to the strength of the Et$_2$O→Al bond. Compound **1-Et$_2$O** therefore provides a "high value" for the Lewis acid-base strength. In a similar approach than Krossing with (ROH)→Al(OR^F)$_3$ adducts, we conducted a broad theoretical comparison of different L→Al(OR^F)$_3$ adducts (see SI for details).[47] Different families of **L** ligands were evaluated: ethers, thioethers, phosphines, phosphine oxide, alkenes as well as solvent molecules (CH$_3$CN and CH$_2$Cl$_2$). The set of calculated adducts was compared to compound **1-PhF** (PhF→Al(OR^F)$_3$, Scheme 5). The goal was to identify L ligands leading to adducts more stable than **1-PhF** but less than **1-Et$_2$O**.

With L=Et$_2$O, the adduct obtained **1-Et$_2$O** (plus one molecule of PhF), is computed more stable by 19.7 kcal.mol^{-1} than **1-PhF** (plus one molecule of Et$_2$O), largely explaining the lack of reactivity observed with **1-Et$_2$O**. The adduct with THF (**1-THF**) is even more stable, by 23.3 kcal.mol^{-1}. Looking for more crowded oxygenated molecules to possibly weaken the O→Al interaction, the Lewis adduct with L = EtO^{t}Bu was computed. Interestingly, it is more stable than **1-PhF** by only 11.4 kcal.mol^{-1} making it a pertinent synthetic target. Adducts with MeO^{t}Bu and O(^{i}Pr)$_2$ were found at -16.0 and -16.6 kcal.mol^{-1} respectively, while the bulkier O(^{t}Bu)$_2$ was computed to be less stable than **1-PhF** (1.1 kcal.mol^{-1}). Finally, the R^{F}OH ligand, featuring the strongly withdrawing C(CF$_3$) kcal.mol^{-1}) did not lead to significant stabilization (-1.4 kcal.mol^{-1}).

The adducts with ligands featuring the softer atom S were calculated to be less stable than their O analogues, in accord with the HSAB theory. For example, while the adduct **1-THF** is 23.3 kcal.mol^{-1} more stable than compound **1-PhF**, the adduct with THT (tetrahydrothiophene) is only 15.7 kcal.mol^{-1} more stable. Among the different "thio" ligands evaluated, the best candidate was identified as di-isopropyl sulfide S^{i}Pr$_2$ that present a stabilization of 13.7 kcal.mol^{-1} compared to the reference **1-PhF**.

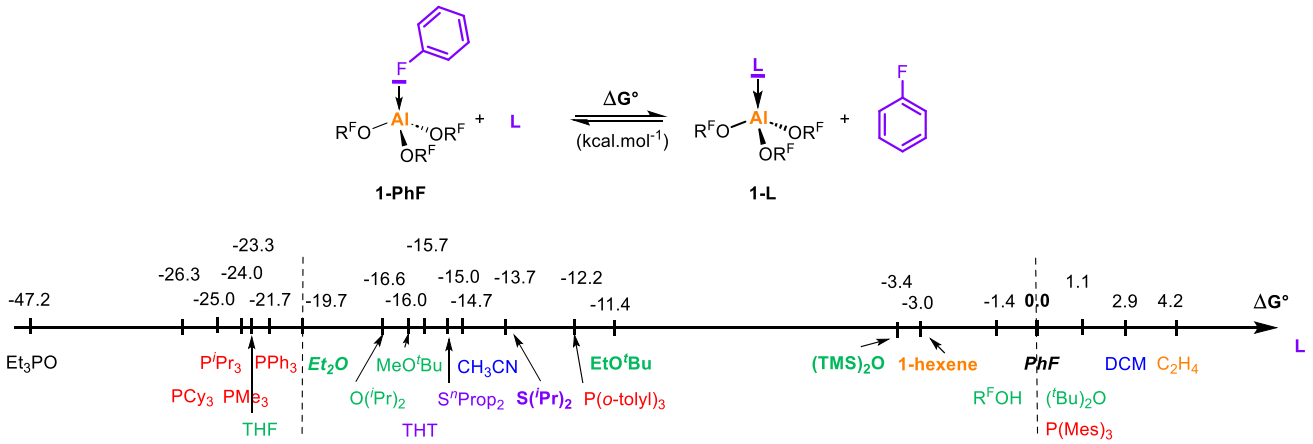

Scheme 5 - Theoretical energy comparison of a series of L→Al(OR^F)$_3$ adducts. Identification of synthetic targets = Compounds in bold.

Alkenes were also considered. The adduct L→Al(OR^F)$_3$ with L = 1-hexene is marginally more stable than **1-PhF** (-3.0 kcal.mol^{-1}) while the adduct with ethylene was less stable (4.2 kcal.mol^{-1}). Their syntheses were envisaged (*vide infra*). We then turned to commercial phosphines. The strongly donating alkyl phosphines PMe_3, P^iPr_3 and PCy_3 gave strong adducts (-24.0, -25.0 and -26.3 kcal.mol^{-1} resp.). Much larger differences of P→Al strength were observed with aryl phosphines. PPh_3 is a much better donor (-21.7 kcal.mol^{-1}) than P(*o*-tolyl)$_3$ (-12.2 kcal.mol^{-1}) itself much stronger than $PMes_3$ (1.1 kcal.mol^{-1}). Finally, solvent adducts were evaluated. The one with CH_3CN was computed to be less stable than **1-Et$_2$O** (-14.7 vs -19.7 kcal.mol^{-1}), making it an interesting species. On the other hand, the CH_2Cl_2 adduct is less stable than **1-PhF** (+2.9 kcal.mol^{-1}), therefore an unsuitable target.

In conclusion of this theoretical investigation, several adducts, featuring EtO^{t}Bu, TMSOTMS, S(^{i}Pr)$_2$, CH_3CN and 1-hexene, were identified as relevant synthetic targets, being both more stable than **1-PhF** (between -3.0 and -14.7 kcal.mol^{-1}) and less stable than **1-Et$_2$O**. Additionally, although predicted less stable ethylene was evaluated to further probe the predictive character of our DFT approach.

Evaluation of synthetic targets. The synthesis of (C$_2$H$_4$)→Al(OR^F)$_3$ was attempted first. Freshly prepared adduct **1-PhF** in fluorobenzene (from $AlEt_3$ and 3.1eq. of R^{F}OH at -35°C, Scheme 6) was placed under an ethylene pressure of 5 bar in an NMR tube. Complete formation of cyclic compound **2** was observed after 16h at RT, attesting decomposition of the Al(OR^F)$_3$ moiety. The decomposition rate of compound **1-PhF** is qualitatively comparable with and without ethylene in the medium. Experimentally, the (C$_2$H$_4$)→Al(OR^F)$_3$ adduct is therefore not significantly more stable than **1-PhF**, which is consistent with DFT calculations (ethylene complex less stable, by 4.2 kcal/mol).

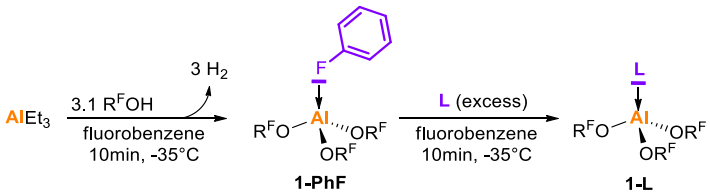

Scheme 6 – General synthetic pathway for the generation of L→Al(OR^F)$_3$ adducts.

The synthesis of the (L)→Al(OR^F)$_3$ adducts, with L = 1-hexene and TMSOTMS, was then considered following the general procedure (Scheme 6). In this case also, formation of cyclic compound **2** was observed after 16h at RT. Despite providing *ca* 3 kcal/mol additional stability vs PhF, these two ligands do not allow extended stability of the adduct. The synthesis of the (EtO^{t}Bu)→Al(OR^F)$_3$ adduct was then considered. When the crude solution was kept at +5°C overnight, colorless crystals were obtained and analyzed by X-Ray diffraction. Although the quality of the crystals was too poor to obtain a satisfactory structure, it nonetheless allowed us to identify the formation of the [(R^{F}O)$_2$Al(μ-OEt)]$_2$ dimeric complex **4** featuring bridging OEt groups as well as only two OR^F moieties per Al center

(see ESI - figure S15). Formation of such species is proposed to result from ligand exchange between $Al(OR^F)_3$ and ^{t}BuOEt, forming ^{t}BuOR^F as by-product.

We then turned our attention to the synthesis of compound **1-S^{i}Pr$_2$** (^{i}Pr$_2$S)→$Al(OR^F)_3$. It was synthesized by the general procedure described on Scheme 6. The complex **1-S^{i}Pr$_2$** was obtained pure after simple evaporation of the volatiles, as shown by elemental analyses. Pleasingly, this complex is stable both in the solid state for extended periods (months) and in solution at room temperature as evidenced by NMR spectroscopy. Crystals of **1-S^{i}Pr$_2$** could be obtained at room temperature from a concentrated toluene solution. A crystal was analyzed by X-ray diffraction (Figure 1). The geometry around the aluminum is distorted tetrahedral (τ_4=0.92).[49] The Al-O distances are similar to those of previously reported adducts.[47,50–55] The Al-S distance (2.359(1)Å) is the shortest reported to our knowledge for a tetracoordinated Al center,[56–59] attesting the strong Lewis acidity of $Al(OR^F)_3$. Being predicted more stable than the S(iPr)$_2$ adduct, and thus less reactive, the CH_3CN one was not evaluated at this stage.

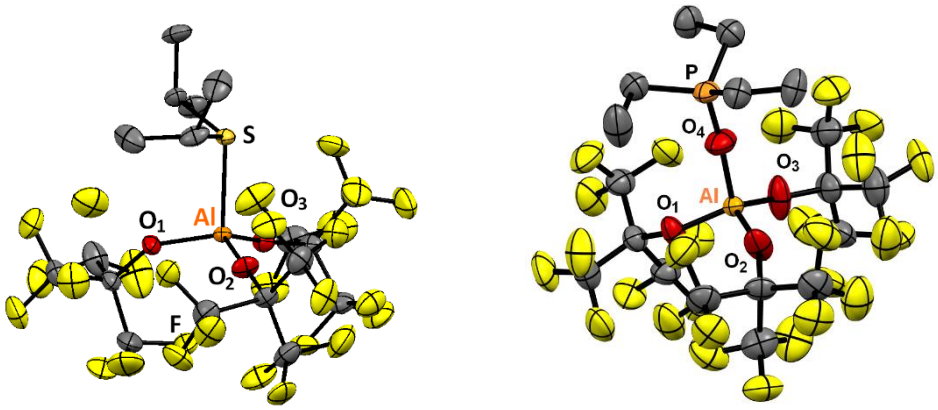

Figure 1 – From left to right: molecular structure of **1-S^{i}Pr$_2$** and **1-OPEt$_3$** in crystalline state. Thermal ellipsoids are drawn at 35% probability. H and disordered atoms, solvent molecule (**1-OPEt3**) are omitted for clarity. Distances [Å] and angles [deg]. **1-S^{i}Pr$_2$** : Al-O_1: 1.698(1), Al-O_2: 1.687(1) ; Al-O_3 : 1.711(1) ; Al-S : 2.359(1) ; Al-$F_{shortest}$: 2.984(8) ; O_1-Al-O_2 : 117.3(1) ; S-Al-O_3 : 102.7(1). **1-OPEt$_3$** : Al-O_1: 1.679(4) ; Al-O_2 : 1.679(4) ; Al-O_3 : 1.687(4) ; Al-O_4 : 1.709(4) ; P-O_4 : 1.505(4) ; Al-$F_{shortest}$: 3.127(18) ; P-O_4-Al : 168.5(4) ; O_4-Al-O_1 : 106.3(2).

Lewis acidity of compound (^{i}Pr$_2$S)→$Al(OR^F)_3$. The Gutmann-Beckett method is one of several methods used to estimate the Lewis acidity of a species, by its coordination to Et_3PO. In short, the measured ^{31}P NMR chemical shift determines the acceptor number (AN) which evaluates the Lewis acidity of the studied compound. Krossing has demonstrated that $Al(OR^F)_3$ is one of the strongest Lewis acid, by calculating its Fluorine Ion Affinity (FIA) thanks to quantum chemical calculations.[52,60] Kögel recently reported that the Guttmann-Beckett method is not appropriate to compare the strength of Al based Lewis acid to related B derivatives.[61] In order to provide additional data on this matter, we synthesized the adduct Et_3PO→$Al(ORF)_3$ **1-OPEt$_3$** following the general strategy. The crystal structure of complex **1-OPEt$_3$** is presented Figure 1. It exhibits a ^{31}P NMR chemical shift at 78.0 ppm in CD_2Cl_2 that lead to a AN of 81.8 for $Al(ORF)_3$. In comparison, $B(C_6F_5)_3$ has an AN of 78.1 (CD_2Cl_2)[62] while $B(OC_6F_5)_3$ (C_6D_6)[63] and $Et_2O.BF_3$ ($CDCl_3$)[64] exhibit respectively an AN of 88.2 and 84.0. $Al(OC\{C_6F_5\}_3)_3$ presents a low AN of 72.7 (supposedly due to steric bulk).[61]

A qualitative, experimental way to probe the donor strength of L to $Al(OR^F)_3$ is to evaluate the remaining Lewis acidity of L→$Al(OR^F)_3$. It can be done via the measurement of the shortest aluminium-fluorine distance ($d_{F\text{-}Al}$) in *trans* position of the Lewis base on the X-ray structure of the adduct under study (Scheme 7). Indeed, if this distance is long, it shows that the $Al(OR^F)_3$ is strongly stabilized by the L donation. On the contrary, if the donation is poor, the $Al(OR^F)_3$ moiety retains significant acidity translated by an Al-F interaction: measured $d_{F\text{-}Al}$ distance is small. In the cases where L=Et_2O (**1-Et$_2$O**), L=THF (**1-THF**) or L=Et_3PO (**1-OPEt$_3$**), the $d_{F\text{-}Al}$ distances are very long at 3.311(8) Å[51], 3.254(3) Å[50] and 3.127(18) Å respectively, showing negligible remaining Lewis acidic character of the Al center. On the other hand, in the adduct **1-PhF**, the distance is short : $d_{F\text{-}Al}$=2.77 Å.[52] For our newly synthesized adduct **1-S^{i}Pr$_2$**, a $d_{F\text{-}Al}$=2.984(8) Å was measured which showed an intermediate remaining Lewis acidity between **1-PhF** and **1-Et$_2$O.**

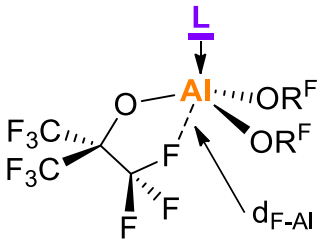

Scheme 7 - Estimation of L→Al(OR^F)$_3$ acidity thanks to the $d_{F\text{-}Al}$ distance.

[OR^F]$^-$ abstraction studies. For this purpose, we first evaluated the abstraction of an [OR^F]$^-$ moiety from (bipyMe$_2$)Ni(OR^F)$_2$ **3**. As mentioned above, reaction of this complex with in situ generated PhF→Al(OR^F)$_3$ allowed such abstraction at room temperature, but did not allow isolation of the corresponding cationic species. Not surprisingly in light of the room temperature stability of (S^{i}Pr$_2$)→Al(OR^F)$_3$ **1-S^{i}Pr$_2$**, its reaction with stoichiometric amounts of **3** in *o*-DFB (ortho-difluorobenzene) at room temperature was very slow (only traces of new signals attributed in ^{1}H NMR after 24h). Interestingly however, when the mixture was heated at 80°C for 5 min., the formation of new compound was observed together with half of the initial compound **3** remaining. Further heating at 80°C for 16 more hours did not lead to significant changes in the ratio of species.

When two equivalents of Lewis acid **1-S^{i}Pr$_2$** were used at 80°C, quantitative conversion of complex **3** was observed (Scheme 8). The formation of a single new complex [(bipyMe$_2$)Ni(OR^F)(^{i}Pr$_2$S)]$^+$[(R^{F}O)$_3$Al-F-Al(OR^F)$_3$]$^-$ was demonstrated by ^{19}F NMR spectroscopy. Indeed, a new signal at +49 ppm (attributed to a new Ni-OR^F fragment) as well as the signals of the known epoxide O(CF$_3$)(C{CF$_3$}$_2$) (t, -70ppm; sept, -110ppm; $^4J_{F\text{-}F}$ = 8.5Hz) and a broad signal at -185 ppm (characteristic of a bridging fluoride between two Al atoms) were observed. The formation of the counter-anion [(R^{F}O)$_3$Al-F-Al(OR^F)$_3$]$^-$ (further noted [Al-F-Al]$^-$) justified the use of two equivalents of **1-S^{i}Pr$_2$**.

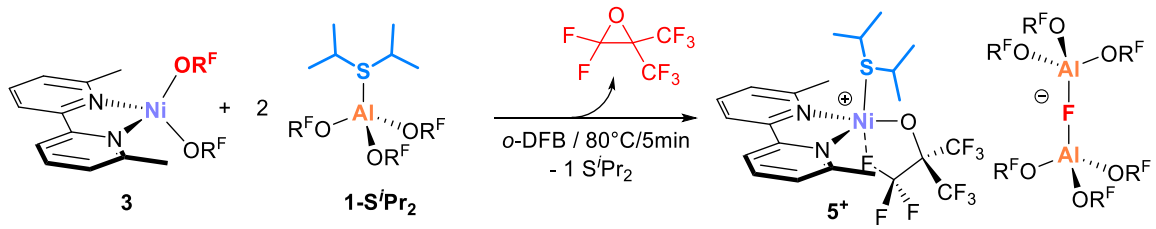

Scheme 8 - Synthesis of compound **5**$^+$[Al-F-Al]$^-$.

The signals of the bipyMe$_2$ ligand, coordinated at a paramagnetic Ni center, were observed between 16 and 82 ppm in the ^{1}H NMR (ESI, figure S8). A broad signal attributed to S^{i}Pr$_2$ was observed at ca 0 ppm, indicating its coordination to the paramagnetic nickel center. Diffusion of Hexamethyldisiloxane (HMDSO) onto the crude mixture in *o*-DFB resulted in the growth of numerous dark red crystals. X-ray diffraction analysis of these single crystals confirmed the structure of compound **5**$^+$[Al-F-Al]$^-$ (cation **5**$^+$ shown Figure 2 left). Interestingly, a strong Ni-F interaction (2.530(2) Å, sum of Van der Waals radii: 1.47 + 1.63 = 3.10 Å) is noted. To our knowledge, this is the first dative F→Ni bond reported in the literature, highlighting the strong Lewis acidity of the metal center. This interaction results in a distorted trigonal bipyramid geometry around the cationic nickel (τ_5=0.40). Despite this F→Ni donation, the corresponding C-F bond is not elongated (1.33 Å). The Ni-O bond (1.873(2) Å) is one of the shortest of all those measured in the L$_2$Ni(OR^F)$_2$ complexes family (1.868(2) Å to 1.937(2) Å).[31,65] Compared to (bipyMe$_2$)Ni(OR^F)$_2$ **3**, the Ni-O bond is only slightly shorter (d_{Ni-O}(**3**) : 1.893(2) vs 1.873(2) for **5**$^+$), showing again the electron deficiency of the nickel center.

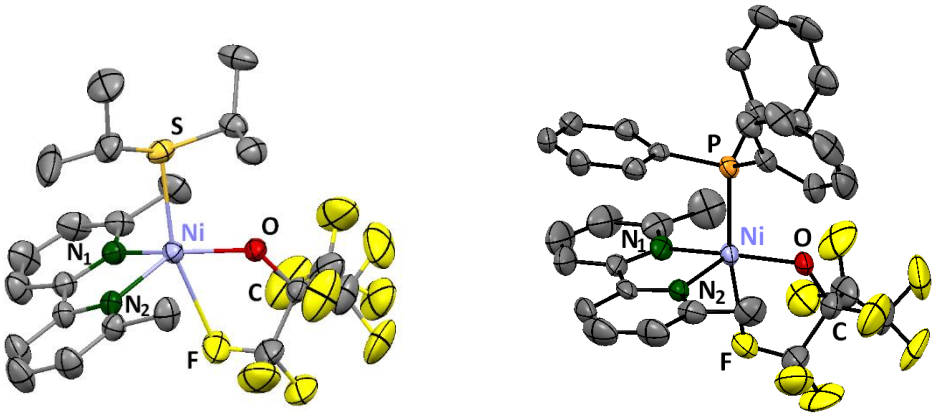

Figure 2 – Left: Molecular structure of **5+**. Thermal ellipsoids are drawn at 50% probability. H and disordered atoms omitted for clarity. Distances [Å] and angles [deg]: Ni-O : 1.873(2) ; Ni-S : 2.369(1) ; Ni-N_1 : 2.010(2) ; Ni-N_2 : 2.008(2) ; Ni-F : 2.530(2) ; S-Ni-F : 162.3(1) ; S-Ni-O : 93.4(1) ; N_1-Ni-N_2 : 81.8(1) ; Ni-O-C : 130.1(1). Right : Molecular structure of the **6**$^+$. Distances [Å] and angles [deg]: Ni-O : 1.881(3) ; Ni-P : 2.344(1) ; Ni-N_1 : 1.994(3) ; Ni-N_2 : 2.004(3) ; Ni-F : 2.561(8) ; S-Ni-F : 166.0(2) ; P-Ni-O : 95.4(2) ; N_1-Ni-N_2 : 83.1(2) ; Ni-O-C : 128.4(4).

Lewis acid **1-S^{i}Pr$_2$** did not present any sign of evolution at 80°C for 24h in o-DFB, which implied involvement of the Ni complex in the formation of the observed by-product and counter ion [Al-F-Al]$^-$. A DFT study rationalized the experimental findings (Scheme 9). The first step consists in the decoordination of S^{i}Pr$_2$ from Al(OR^F)$_3$ (**TS$_{A-B}$** of 26.5 kcal.mol^{-1}). The released Lewis acid then activates a C-F bond of an [OR^F]$^-$ ligand via an endergonic reaction (15.1 kcal.mol^{-1}), however kinetically accessible. Indeed, in adduct **C**, the length of the C-F bond activated by the Al center is 1.44 Å, which is 0.11 Å longer than classical C-F bonds. This interaction favors the nucleophilic substitution which leads to the cationic compound **D** comprising the coordinated epoxide O(CH$_2$)(C{CF$_3$}$_2$) and the counter-anion [(R^{F}O)$_3$AlF]$^-$. The **TS$_{C-D}$** transition state that links these two compounds (**C** and **D**) is located at 31.7 kcal.mol^{-1} in G, in qualitative agreement with the required experimental conditions (abstraction at 80°C), although being rather high. From **D**, the substitution of the electron poor epoxide by the thioether in the nickel coordination sphere is favorable. The complex **E** is indeed located at -3.9 kcal.mol^{-1} (25.6 kcal.mol^{-1} lower than **D**). The coordination of [(R^{F}O)$_3$AlF]$^-$ on Al(OR^F)$_3$ from **E** lead to the formation of **F** (**5**) which is the most stable complex of the study (-9.0 kcal.mol^{-1}), supporting the mechanistic pathway we propose.

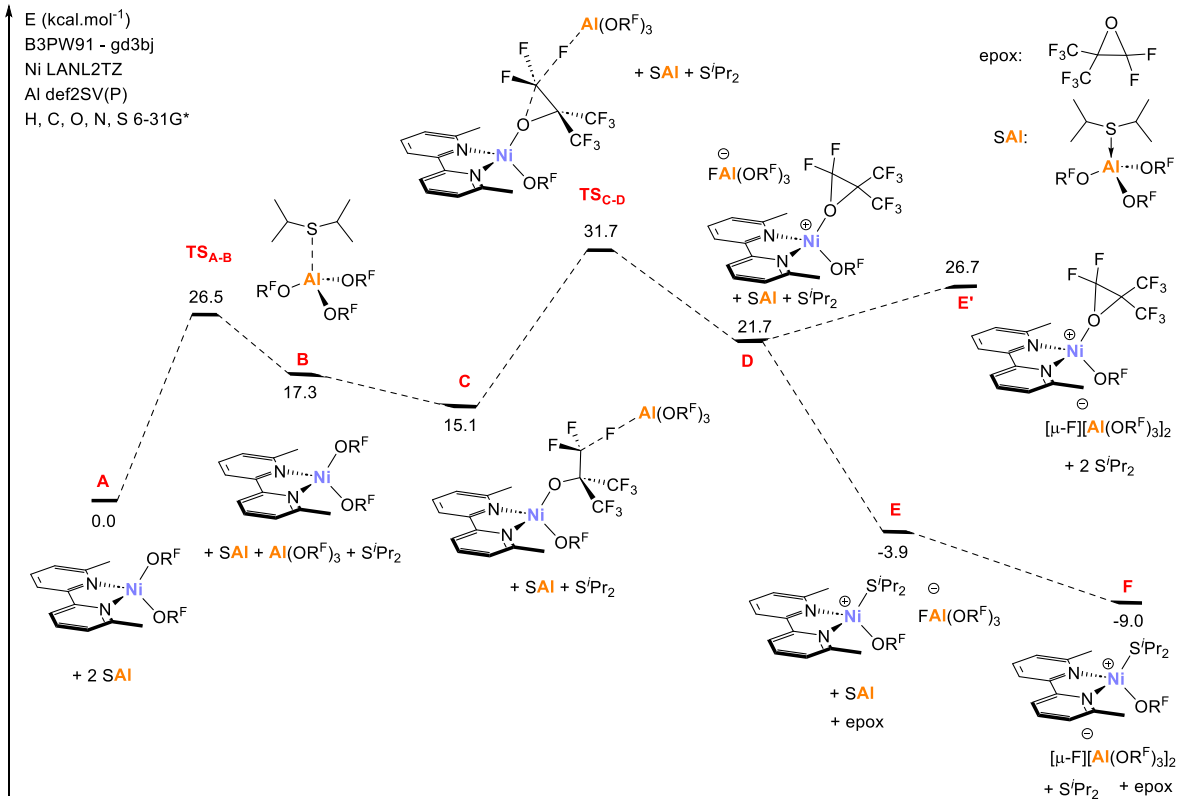

Scheme 9 – PES for the formation of **5**$^{+}$ [Al-F-Al]$^{-}$.

Reactivity of complex 5^{+}. As mentioned above, complex **5**$^{+}$ appeared to be quantitatively obtained from NMR analyses of the crude mixture, and readily crystallized. However, we were unable to fully characterize it without formation of very minor impurities, which we propose to come from the lability of the thioether ligand. Indeed, if cationic complex **5**$^{+}$ is stable and soluble in *o*-DFB and DCM, it decomposes to unknown products in THF and ACN.It is not stable towards water traces as well (see ESI – figure S16). In order to obtain a more stable complex, one eq. of Ph_3P was added to the crude solution containing **5**$^{+}$. It formed the desired ionic complex [(bipyMe$_2$)Ni(OR^F)(PPh$_3$)][Al-F-Al] **6**$^{+}$[Al-F-Al]$^{-}$ (Scheme 10). In the ^{1}H NMR spectrum, broad signals at -6 and +23 ppm were attributed to Ph_3P coordinated on the paramagnetic nickel. The signals of the bipyMe$_2$ ligand were also shifted. In ^{19}F NMR, the signals of the [Al-F-Al]$^{-}$ counter-anion remained unchanged while a new signal at +105 ppm was detected. The signal at +49ppm of starting complex **5**$^{+}$ was no longer present. Finally, no ^{31}P NMR signal was observed, attesting the coordination of Ph_3P on Ni. Yellow crystals could be grown thanks to HMDSO diffusion in the crude medium within 24 h. Single crystal XRD analysis confirmed the structure of complex **6**$^{+}$[Al-F-Al]$^{-}$ (Figure 2, right). The geometry around the nickel is very similar to that of complex **5**$^{+}$[Al-F-Al]$^{-}$ (τ_5 = 0.54). Compared to the latter, the Ni-O and Ni-N distances are almost identical. The angles are similar. The Ni-F interaction is slightly elongated, (Ni-F 2.561(8) Å vs Ni-F : 2.530 (2) Å in **5**$^{+}$) highlighting the better stabilization of cationic nickel by phosphine compared to sulfide. In contrast, the Ni-P bond length is very long (2.344(1) Å) compared to Ni-P lengths in other [(Ph_3P)NiL$_n$]$^{+}$ tetrahedral complexes (from 2.18 to 2.21 Å).[66,67]

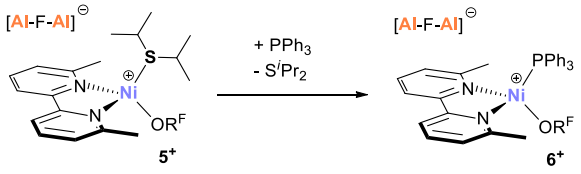

Scheme 10 – Thioether ligand displacement by PPh_3.

This long Ni-P bond indicates a mismatch between the strong acidity of Ni (hard cation) and the basicity of P (soft base). This behavior could be interesting for a possible reactivity with a potentially easy displacement of the phosphine. In conclusion, complex $[(bipyMe_2)Ni(OR^F)(S^iPr_2)]^+$ **5**$^+$ can serve as a precursor to other complexes via facile S^iPr_2 displacement.

Reactivity between (bipyMe$_2$)NiCl$_2$ and 1-S^{i}Pr$_2$.

Finally, in order to evaluate the benefits of using $[OR^F]^-$ ligands compared to halogen ligands, the abstraction of chloride ligand with the Lewis adduct **1-S^{i}Pr$_2$** was studied. The addition of one equivalent of **1-S^{i}Pr$_2$** was added to the $(bipyMe_2)NiCl_2$ complex **7** at RT in *o*-DFB which led to complete dissolution within 30min (Scheme 11).

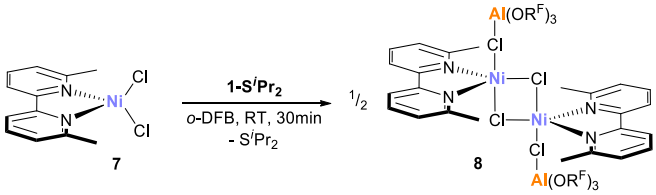

Scheme 11 – Synthesis of complex **8** from complex **7** and **1-S^{i}Pr$_2$**.

In ^{1}H NMR, the formation of a paramagnetic nickel complex with the $bipyMe_2$ ligand was observed as well as the free S^iPr_2 ligand. In ^{19}F NMR, only a signal at -75ppm was present. The diffusion of pentane on the crude solution in *o*-DFB allowed crystallization of orange crystals which were analyzed by XRD. The structure of dimeric complex **8** $[(bipyMe_2)Ni\{ClAl(OR^F)_3\}(\mu Cl)]_2$ is shown in Figure 3. The Ni-Cl_2 bond is strongly elongated (2.50 Å vs 2.26 Å and 2.38 Å for Ni-Cl_1 and Ni-Cl_1' respectively), due to the presence of the Lewis acid $Al(OR^F)_3$. The Al-Cl_2 bond at 2.20 Å is comparable to the Al-Cl distance in the $[ClAl(OR^F)_3]^-$ counterion.[61] This shows that complex **8** is a zwitterionic species with the $[ClAl(OR^F)_3]^-$ counterion coordinated on the cationic nickel. Interestingly, the chloro aluminate counter anion is therefore a better ligand than the sulfide S^iPr_2, that remains in solution.

The formation of complex **8** $[(bipyMe_2)Ni\{ClAl(OR^F)_3\}(\mu Cl)]_2$ rather than $[(bipyMe_2)Ni(Cl)(^iPr_2S)]^+[AlCl]^-$ clearly illustrates the advantage of using a "$Ni(OR^F)$" moiety in conjunction with $Al(OR^F)_3$. The strength of the Al-F bond *vs* Al-Cl provides the driving force for abstraction of OR^F from the metal center, thereby creating the desired vacant coordination site.

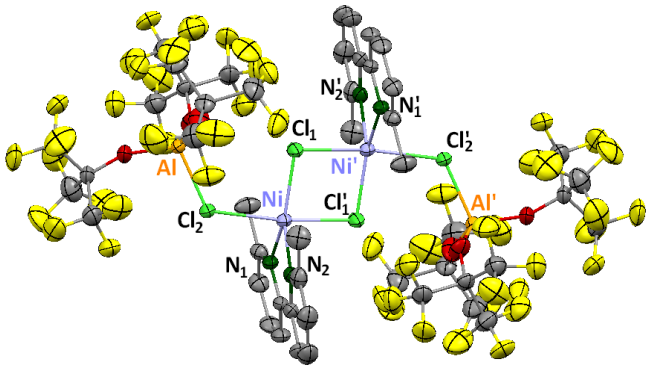

Figure 3 – Molecular structure of **8** in crystalline state. Thermal ellipsoids are drawn at 50% probability. H and disordered atoms are omitted for clarity. Distances [Å] and angles [deg]: Ni-N_1 : 1.997(2) ; Ni-N_2 : 2.013(2) ; Ni-Cl_1 : 2.255(1) ; Ni-Cl'$_1$: 2.386(1) ; Ni-Cl_2 : 2.499(1) ; Al-Cl_2 : 2.201(1) ; Cl_1-Ni-Cl_2 : 89.08(2) ; Cl_1-Ni-Cl_1' : 84.98(2) ; N_1-Ni-N_2 : 81.39(8) ; Cl_2-Ni-Cl_1' : 171.74(3).

Conclusion

A predictive DFT study has allowed the identification of several potential "stable yet reactive" L→Al(OR^F)$_3$ complexes that could act as masked precursors of one of the most potent Lewis acids Al(OR^F)$_3$. The adduct ^{i}Pr$_2$S→Al(OR^F)$_3$ **1-S^{i}Pr$_2$** was then synthesized, which enabled testing the novel strategy to generate a vacant coordination site at a metal center: abstraction of OR^{F-} ligand from M-OR^F by Al(OR^F)$_3$. Starting from (bipyMe$_2$)Ni(OR^F)$_2$, the ionic [(bipyMe$_2$)Ni(OR^F)(S^{i}Pr$_2$)]$^+$[(R^FO)$_3$Al-F-Al(OR^F)$_3$]$^-$ complex is formed upon reaction with ^{i}Pr$_2$S→Al(OR^F)$_3$. The mechanism was rationalized by DFT calculations. It relies on the abstraction of a fluoride anion of the Ni-OR^F to form the per-fluorinated epoxide O(CF$_2$)C(CF$_3$)$_2$. Importantly for subsequent reactivity at the Ni center, the thioether ligand is readily displaced by PPh$_3$ or H$_2$O. The method developed in this work, involving abstraction of [OR^F]$^-$ by Al(OR^F)$_3$, could allow access to many coordinatively unsaturated cations, and thus to exacerbated reactivity.

Experimental Section

General Procedure: All the reactions were carried out in a glove box or using standard Schlenk techniques under N$_2$. All commercial compounds were put under inert atmosphere before use. Compound **3**, (bipyMe$_2$)Ni(OR^F)$_2$, was synthesized according to our previously reported procedure.[65] All solvents, except *o*-DFB, were taken from MBSPS-800 solvent purification system, then degassed and further dried using molecular sieves. *o*-DFB was pre-dried over CaH$_2$ and then filtered and stored on molecular sieves. ^{1}H, ^{13}C, ^{19}F and ^{31}P NMR spectra were recorded on Bruker Avance 300 and 400 MHz spectrometers. ^{1}H and ^{13}C chemical shifts reported are referenced internally to used solvent while ^{19}F and ^{31}P chemical shifts are referenced to an external standard of trichlorofluoromethane and phosphoric acid respectively. Elemental analysis was carried out by combustion analysis using vario MICRO cube apparatus from Elementar. HRMS analyses were conducted with "QTOF Impact II - Bruker / UHPLC U3000 chain – Dionex" spectrometer. A cryospray (Cold Spray Ionization) source is used to detect exact masses.[68] X-ray intensity data were collected at 193 K on a Bruker-AXS D8-VENTURE diffractometer (**4, 1-S^{i}Pr$_2$, 1-OPEt$_3$, 5, 5-H$_2$O, 6[Al(OR^F)$_4$]** and **8**) equipped with a Mo Kα sealed tube (λ = 0.71073 Å), a multilayer TRIUMPH X-Ray mirror and a Photon III-C14 detector or at 153 K on a Bruker-AXS kappa APEX II Quazar diffractometer (**6[Al-F-Al]**) equipped with a 30W air-cooled microfocus source using Mo Kα radiation (**8**). The semi-empirical absorption corrections were employed.[69] The structures were solved using an intrinsic phasing method,[70] and refined by full matrix least squares procedures on F^2.[71] All non-H atoms were refined with anisotropic displacement parameters. Hydrogen atoms were refined isotropically at calculated positions using a riding model with their isotropic displacement parameters constrained to be equal to 1.5 times the equivalent isotropic displacement parameters of their pivot atoms for terminal sp3 carbon and 1.2 times for all other carbon atoms. CCDC-2218595 (**4**), CCDC-2218596 (**1-S^{i}Pr$_2$**), CCDC-2218597 (**1-OPEt$_3$**), CCDC-2218598 (**5**), CCDC-2218599 (**5-H$_2$O**), CCDC-2218600 (**6[Al(OR^F)$_4$]**), CCDC-2218601 (**6[Al-F-Al]**) and CCDC-2218602 (**8**) contain the supplementary crystallographic data. These data can be obtained free of charge from https://www.ccdc.cam.ac.uk/structures/ or from the Cambridge Crystallographic Data Centre, 12 Union Road, Cambridge CB2 1EZ, UK; tel: + 44 (0)1223 336408; fax: + 44 (0)1223336033; or e-mail: deposit@ccdc.cam.ac.uk

Preparation of ^{i}Pr$_2$S→Al(OR^F)$_3$ 1-S^{i}Pr$_2$: solution of per-fluoro-tert-butanol (0.65mL, 4.66mmol, 4.9 eq.) in fluorobenzene (3mL) was added at -20°C onto a solution of AlEt3 (0.5ml, 1.9M in toluene, 0.95mmol, 1 eq.) in fluorobenzene (3mL). A gas release was observed at once (ethane). The mixture was allowed to react 10min at -35°C. A solution of di-isopropyl sulphide (0.15 mL, 1.03mmol, 1.1 eq.) in fluorobenzene (2mL) was added to the previous mixture, still at -35°C. The mixture was allowed to warm up to RT. Solvent was removed under reduced pressure which removed both the excess of SiPr2 and the excess of alcohol. The obtained white solid (750mg, 93%) does not need further purification as attested by the results of the elemental analysis and can be stored at RT under inert atmosphere for a long period (months). Crystals were obtained from a saturated solution in toluene or from diffusion of heptane in a solution of the compound in fluorobenzene. **^{1}H NMR** (298K, 300,0MHz, C$_6$D$_6$): 0.94 (d, J = 6.90Hz, 12H, CH$_3$), 3.22 (sept., J = 6.90Hz, 2H, CHMe$_2$) ppm. **^{13}C{^{1}H}{^{31}P}** NMR (298K, 75 MHz, C$_6$D$_6$): 22.23 (s, CH$_3$), 39.06 (s, CH), 121.32 (q, $J_{C\text{-}F}$ = 292Hz, CF$_3$) ppm. **^{19}F{^{1}H} NMR** (298K, 282 MHz, C$_6$D$_6$): -74.8 (s, C(CF$_3$)$_3$) ppm. EA: Anal. Calc for C$_{18}$H$_{14}$AlF$_{27}$O$_3$S: C, 25.43; H, 1.66. Found: C, 25.19; H,1.17.

Preparation of Et$_3$PO→Al(OR^F)$_3$ 1-Et$_3$PO: A solution of Et$_3$PO (15.8mg, 0.12mmol, 1eq.) in fluorobenzene (5mL) was added onto a solution of (^{i}Pr$_2$S)→Al(OR^F)$_3$ (100mg, 0.12mmol, 1eq.) in fluorobenzene (5mL). The mixture was allowed to react 30min at RT. Solvent was then removed under reduced pressure to afford a white solid which was extensively dried under reduced pressure. The obtained white solid (92mg, 90%) does not need further purification and can be stored at RT under inert atmosphere for long periods (months). Crystals were obtained from a saturated solution of deuterated benzene. **^{1}H NMR** (298K, 500MHz, CD$_2$Cl$_2$): 1.20 (d of t, $J_{H\text{-}H}$=7.7 Hz, $J_{P\text{-}H}$=18.5 Hz, 9H, CH$_3$), 1.95 (d of q, $J_{H\text{-}H}$=7.7 Hz, $J_{P\text{-}H}$=11.8 Hz, 6H, CH$_2$) ppm. **^{13}C{^{1}H} NMR** (298K, 125.7 MHz, CD$_2$Cl$_2$): 4,68 (d, $J_{C\text{-}P}$=5.1 Hz CH$_3$), 17.94 (d, JC-P=66.5 Hz, CH$_2$) 121.59 (q, $J_{C\text{-}F}$=292Hz, CF3) ppm. **^{19}F{^{1}H} NMR** (298K, 470.6 Hz, CD$_2$Cl$_2$): -75.6 (s, C(CF$_3$)$_3$) ppm. **^{31}P{^{1}H} NMR** (298K, 202.4 Hz, CD$_2$Cl$_2$): 78.0 (s) ppm. **HRMS** (TOF): Calc. for (Et$_3$PO)Al(OR^F)$_2$ = C$_{14}$H$_{15}$AlO$_3$F$_{18}$P 631.0287 ; found 631.0291.

Preparation of [(bipyMe$_2$)Ni(OR^F)(S^{i}Pr$_2$)][Al-F-Al] 5 : To a solution of (6,6'-dimethyl-2,2'-bipyridine)Ni(OR^F)$_2$ (100 mg, 0.14 mmol, 1eq.) in *o*-DFB (3mL), a solution of (^{i}Pr$_2$S)→Al(OR^F)$_3$ (238.5 mg, 0.28 mmol, 2eq.) in *o*-DFB (3mL) was added dropwise. The mixture was heated at 80°C during 5min. The solution, which remained orange, was concentrated to 2mL. A layer of HMDSO (3mL) was slowly added on the crude mixture. After 48h of diffusion at 25°C, deep red crystals suitable for X-Ray diffraction analyses were obtained. **^{1}H NMR** (298K, 300,0MHz, *o*-DFB): -2.22 – 2.77 (br, S^{i}Pr$_2$, n x 14H), 16.08 (s, bipyMe$_2$-ArH, 2H), 37.70 (br, bipyMe$_2$-CH$_3$, 6H), 55.11 (s, bipyMe$_2$-ArH, 2H) 82.59 (s, bipyMe$_2$-ArH, 2H) ppm**. ^{19}F{^{1}H} NMR** (298K, 282,2 Hz, *o*-DFB): +52 (s, Ni-O-C(CF$_3$)$_3$, 9F), -75 (s, Al-O-C(CF$_3$)$_3$, 54F), -184ppm (br, Al-F-Al, 1F) ppm.

Preparation of [(bipyMe$_2$)Ni(OR^F)(PPh$_3$)][Al-F-Al] 6 : To a solution of (6,6'-dimethyl-2,2'-bipyridine)Ni(OR^F)$_2$ (100mg, 0.14 mmol, 1eq.) in *o*-DFB (3mL), a solution of (^{i}Pr$_2$S)→Al(OR^F)$_3$ (238.5 mg, 0.28 mmol, 2eq.) in *o*-DFB (3mL) was added dropwise. The mixture was heated at 80°C during 5min. A solution of Ph$_3$P (36.8 mg, 0.14 mmol, 1 eq.) in *o*-DFB (3mL) was added on the previous mixture. The solution became bright yellow at once. The solution was concentrated to 2mL and a layer of HMDSO (3mL) was slowly added. After 48h of diffusion at 25°C, deep red crystals suitable for X-Ray diffraction analyses were obtained. **^{1}H NMR** (298K, 300,0MHz, *o*-DFB): -8.36 – -4.84 (br, Ph$_3$P-ArH, 10H), 17.95 (br, bipyMe$_2$-CH$_3$, 6H), 22.70 (br, Ph$_3$P-Ar-H, 5H), 45.48 (s, bipyMe$_2$-ArH, 2H), 75.22 (s, bipyMe$_2$-ArH, 2H) ppm. **^{19}F{^{1}H} NMR** (298K, 282,2 Hz, *o*-DFB): +105 (s, Ni-O-C(CF$_3$)$_3$, 9F), -75 (s, Al-O-C(CF$_3$)$_3$, 54F), -184ppm (br, Al-**F**-Al, 1F) ppm. **HRMS** (CSI): calc. for [(bipyMe$_2$)Ni(OR^F)(PPh$_3$)]$^+$= $C_{34}H_{27}F_9N_2NiOP^+$ 739.1066 ; found 739.1067.

Preparation of [(bipyMe$_2$)Ni{ClAl(OR^F)$_3$}(μ-Cl)]$_2$ 8 : A solution of **1-S^{i}Pr$_2$** (271mg, 0.32mmol, 1eq.) in *o*-DFB (3mL) was added onto a suspension (bipyMe$_2$)NiCl$_2$ (100mg, 0.32mmol, 1eq.) in *o*-DFB (3mL). The mixture was heated at 50°C for 1h under stirring. A deep orange solution was obtained (NMRs of the crude presented below). The solution was concentrated to half of its initial volume and HMDSO was added for diffusion. After one day, deep orange crystals had formed and were analyzed by X-Ray diffraction. Upon dissolution of the crystals for analysis purposes in *o*-DFB, ^{1}H NMR show several "(bipyMe$_2$)Ni" fragments. On the other hand, unidentified signals around -75ppm are systematically observed in ^{19}F NMR. **^{1}H NMR** (298K, 300,0MHz, *o*-DFB): 16.32 (br, Ar-H), 24.07 (br, CH$_3$), 57.00 (br, Ar-H), 79.11 (br, Ar-H) ppm. **^{19}F{^{1}H} NMR** (298K, 282,2 Hz, *o*-DFB): -76 (s, Al-O-C(CF$_3$)$_3$) ppm.

Computational details. Geometry optimization were performed using Gaussian 09 (Revision D01)[72] at the B3PW91 level of hybrid density functional theory,[73,74] adding D3(bj) corrections.[75,76] The geometries of all optimized structures are given in the .xyz file attached to the publication. Frequency calculations on optimized geometries ensured that structures were minima (zero imaginary frequencies). The Ni atoms were represented by a LANL2TZ basis set.[77,78] The Al atoms were represented with the def2SV(P) basis set.[79] All other atoms (H, C, N, O, F, S) were represented by a 6-31G* basis set.[80–84]

Acknowledgements

For financial support of this work, we acknowledge CNRS, Université Paul Sabatier Toulouse, and IFP Energies Nouvelles. CALMIP is gratefully acknowledged for the access to the supercomputing facilities.

Keywords: Alkoxide • Aluminium • DFT • Lewis superacid • Nickel

[1] K. Izod, P. Evans, P. G. Waddell, *Angew. Chemie - Int. Ed.* **2019**, *58*, 11007–11012.

[2] R. Schowner, I. Elser, M. Benedikter, M. Momin, W. Frey, T. Schneck, L. Stöhr, M. R. Buchmeiser, *Angew. Chemie - Int. Ed.* **2020**, *59*, 951–958.

[3] T. Agapie, J. A. Labinger, J. E. Bercaw, *J. Am. Chem. Soc.* **2007**, *129*, 14281–14295.

[4] A. M. Camp, M. R. Kita, P. T. Blackburn, H. M. Dodge, C. H. Chen, A. J. M. Miller, *J. Am. Chem. Soc.* **2021**, *143*, 2792–2800.

[5] H. S. Sam Chan, Q. N. N. Nguyen, R. S. Paton, J. W. Burton, *J. Am. Chem. Soc.* **2019**, *141*, 15951–15962.

[6] P. Dabringhaus, M. Schorpp, H. Scherer, I. Krossing, *Angew. Chemie - Int. Ed.* **2020**, *59*, 22023–22027.

[7] S. Bennaamane, M. F. Espada, I. Yagoub, N. Saffon-Merceron, N. Nebra, M. Fustier-Boutignon, E. Clot, N. Mézailles, *Eur. J. Inorg. Chem.* **2020**, *2020*, 1499–1505.

[8] M. F. Espada, S. Bennaamane, Q. Liao, N. Saffon-Merceron, S. Massou, E. Clot, N. Nebra, M. Fustier-Boutignon, N. Mézailles, *Angew. Chemie - Int. Ed.* **2018**, *57*, 12865–12868.

[9] I. Krossing, *Chem. - A Eur. J.* **2001**, *7*, 490–502.

[10] I. Krossing, H. Brands, R. Feuerhake, S. Koenig, in *J. Fluor. Chem.*, **2001**.

[11] A. Decken, H. D. B. Jenkins, G. B. Nikiforov, J. Passmore, *Dalt. Trans.* **2004**, 2496–2504.

[12] I. Krossing, A. Reisinger, *Eur. J. Inorg. Chem.* **2005**, 1979–1989.

[13] T. A. Engesser, C. Friedmann, A. Martens, D. Kratzert, P. J. Malinowski, I. Krossing, *Chem. - A Eur. J.* **2016**, *22*, 15085–15094.

[14] I. M. Riddlestone, A. Kraft, J. Schaefer, I. Krossing, *Angew. Chemie - Int. Ed.* **2018**, *57*, 13982–14024.

[15] I. Krossing, I. Raabe, *Angew. Chemie - Int. Ed.* **2004**, *43*, 2066–2090.

[16] T. A. Engesser, M. R. Lichtenthaler, M. Schleep, I. Krossing, *Chem. Soc. Rev.* **2016**, *45*, 789–799.

[17] J. F. Hartwig, in *Organotransition Met. Chem. From Bond. to Catal.*, **2010**, pp. 147–216.

[18] D. C. Bradley, R. C. Mehrota, I. P. Rothwell, A. Singh, *Alkoxo and Aryloxo Derivatives of Metals*, Academic Press, **2001**.

[19] H. W. Roesky, S. Singh, K. K. M. Yusuff, J. A. Maguire, N. S. Hosmane, *Chem. Rev.* **2006**, *106*, 3813–3843.

[20] H. E. Bryndza, W. Tam, *Chem. Rev.* **1988**, *88*, 1163–1188.
[21] K. A. Moltved, K. P. Kepp, *J. Phys. Chem. C* **2019**, *123*, 18432–18444.
[22] H. E. Bryndza, L. K. Fong, R. A. Paciello, W. Tam, J. E. Bercaw, *J. Am. Chem. Soc.* **1987**, *109*, 1444–1456.
[23] J. Cornella, E. Gómez-Bengoa, R. Martin, *J. Am. Chem. Soc.* **2013**, *135*, 1997–2009.
[24] J. A. Bellow, M. Yousif, D. Fang, E. G. Kratz, G. A. Cisneros, S. Groysman, *Inorg. Chem.* **2015**, *54*, 5624–5633.
[25] J. Campora, P. Palma, D. del Rio, M. M. Conego, E. Alvarez, *Organometallics* **2004**, *23*, 5653–5655.
[26] P. T. Matsunaga, J. C. Mavropoulos, G. L. Hillhouse, *Polyhedron* **1995**, *14*, 175–185.
[27] N. M. N. M. Otbu, N. Bu, A. K. Mcmullen, T. D. Tilley, A. L. Rheingold, S. J. Geib, *Inorg. Chem.* **1990**, *29*, 2228–2232.
[28] R. T. Boeré, C. D. Montgomery, N. C. Payne, C. J. Willis, *Inorg. Chem.* **1985**, *24*, 3680–3687.
[29] J. Cámpora, I. Matas, P. Palma, C. Graiff, A. Tiripicchio, *Organometallics* **2005**, *24*, 2827–2830.
[30] M. Kim, L. N. Zakharov, A. L. Rheingold, L. H. Doerrer, *Polyhedron* **2005**, *24*, 1803–1812.
[31] S. E. N. Brazeau, F. Pope, V. L. Huang, C. Anklin, A. L. Rheingold, L. H. Doerrer, *Polyhedron* **2020**, *186*, 114609.
[32] L. J. Treadwell, T. J. Boyle, W. A. Phelan, M. V. Parkes, D. P. Young, *Dalt. Trans.* **2017**, *46*, 5806–5815.
[33] L. M. Martínez-Prieto, P. Palma, E. Álvarez, J. Cámpora, *Inorg. Chem.* **2017**, *56*, 13086–13099.
[34] L. M. Martínez-Prieto, J. Cámpora, *Isr. J. Chem.* **2020**, *60*, 373–393.
[35] L. M. Martínez-Prieto, P. Palma, J. Cámpora, *Dalt. Trans.* **2019**, *48*, 1351–1366.
[36] S. Oh, S. Kim, D. Lee, J. Gwak, Y. Lee, *Inorg. Chem.* **2016**, *55*, 12863–12871.
[37] Y. E. Kim, S. Oh, S. Kim, O. Kim, J. Kim, S. W. Han, Y. Lee, *J. Am. Chem. Soc.* **2015**, *137*, 4280–4283.
[38] L. M. Martínez-Prieto, D. del Río, E. Álvarez, P. Palma, J. Cámpora, *Eur. J. Inorg. Chem.* **2021**, 2958–2975.
[39] C. Yao, P. Chakraborty, E. Aresu, H. Li, C. Guan, C. Zhou, L. C. Liang, K. W. Huang, *Dalt. Trans.* **2018**, *47*, 16057–16065.
[40] S. Bertini, M. Albrecht, *Organometallics* **2020**, *39*, 3413–3424.
[41] A. Correa, T. Leon, R. Martin, *J. Am. Chem. Soc* **2014**, *136*, 1062–1069.
[42] S. A. Derhamine, T. Krachko, N. Monteiro, G. Pilet, J. Schranck, A. Tlili, A. Amgoune, *Angew. Chemie - Int. Ed.* **2020**, *59*, 18948–18953.
[43] R. M. Oechsner, J. P. Wagner, I. Fleischer, *ACS Catal.* **2022**, *12*, 2233–2243.
[44] J. P. Cloutier, F. Zamani, D. Zargarian, *New J. Chem.* **2022**, *46*, 1800–1807.
[45] T. Gunasekara, Y. Tong, A. L. Speelman, J. D. Erickson, A. M. Appel, M. B. Hall, E. S. Wiedner, *ACS Catal.* **2022**, *12*, 2729–2740.
[46] C. A. Malapit, M. Borrell, M. W. Milbauer, C. E. Brigham, M. S. Sanford, *J. Am. Chem. Soc.* **2020**, *142*, 5918–5923.
[47] A. Kraft, N. Trapp, D. Himmel, H. Böhrer, P. Schlüter, H. Scherer, I. Krossing, *Chem. - A Eur. J.* **2012**, *18*, 9371–9380.
[48] D. S. Mcguinness, A. J. Rucklidge, R. P. Tooze, A. M. Z. Z. Slawin, *Organometallics* **2007**, *26*, 2561.
[49] L. Yang, D. R. Powell, R. P. Houser, *J. Chem. Soc. Dalt. Trans.* **2007**, 955–964.
[50] A. Bihlmeier, M. Gonsior, I. Raabe, N. Trapp, I. Krossing, *Chem. - A Eur. J.* **2004**, *10*, 5041–5051.
[51] D. S. McGuinness, A. J. Rucklidge, R. P. Tooze, A. M. Z. Slawin, *Organometallics* **2007**, *26*, 2561–2569.
[52] L. O. Müller, D. Himmel, J. Stauffer, G. Steinfeld, J. Slattery, G. Santiso-Quiñones, V. Brecht, I. Krossing, *Angew. Chemie - Int. Ed.* **2008**, *47*, 7659–7663.
[53] M. Tohde, L. O. Müller, D. Himmel, H. Scherer, I. Krossing, Chem. Eur. J. **2014**, 20, 1218–1222.
[54] A. Martens, P. Weiss, M. C. Krummer, M. Kreuze, A. Meierhöfer, S. C. Meier, J. Bohnenberg, H. Scherer, I. Riddlestone, I. Krossing, Chem. Sci. **2018**, 9, 7058–7068.
[55] A. Martens, O. Peterson, H. Scherer, I. Riddlestone, I. Krossing, Organometallics **2018**, 37, 706–711.
[56] G. H. Robinson, S. A. Sangokoya, *J. Am. Chem. Soc.* **1988**, *110*, 1494–1497.
[57] R. T. Tjahjanto, M. F. Peintinger, T. Bredow, J. Beck, *Eur. J. Inorg. Chem.* **2012**, 3625–3635.
[58] G. H. Robinson, H. Zhang, J. L. Atwood, **1987**, *6*, 887–889.
[59] K. George, M. Jura, W. Levason, M. E. Light, G. Reid, *Dalt. Trans.* **2014**, *43*, 3637–3648.
[60] P. Erdmann, J. Leitner, J. Schwarz, L. Greb, *ChemPhysChem* **2020**, *21*, 987–994.
[61] J. F. Kögel, A. Y. Timoshkin, A. Schröder, E. Lork, J. Beckmann, *Chem. Sci.* **2018**, *9*, 8178–8183.
[62] A. E. Ashley, T. J. Herrington, G. G. Wildgoose, H. Zaher, A. L. Thompson, N. H. Rees, T. Krämer, D. Öhare, *J. Am. Chem. Soc.* **2011**, *133*, 14727–14740.
[63] G. J. P. Britovsek, J. Ugolotti, A. J. P. White, *Organometallics* **2005**, *24*, 1685–1691.

[64] E. L. Myers, C. P. Butts, V. K. Aggarwal, *Chem. Commun.* **2006**, 4434–4436.

[65] J. Petit, N. Saffon-Merceron, L. Magna, N. Mézailles, *Organometallics* **2021**, *40*, 4133–4142.

[66] F. Koch, A. Berkefeld, H. Schubert, C. Grauer, *Chem. - A Eur. J.* **2016**, *22*, 14640.

[67] F. Koch, A. Berkefeld, B. Speiser, H. Schubert, *Chem. - A Eur. J.* **2017**, *23*, 16681.

[68] K. Yamaguchi, *J. Mass Spectrom.* **2003**, *38*, 473–490.

[69] U. Bruker, SADABS, Bruker AXS Inc., Madison, Wisconsin, **2008**.

[70] G. M. Sheldrick, *Acta Crystallogr. Sect. A Found. Crystallogr.* **2015**, *71*, 3–8.

[71] G. M. Sheldrick, *Acta Crystallogr. Sect. A Found. Crystallogr.* **2008**, *A64*, 112–122.

[72] Frisch, M. J.; Trucks, G. W.; Schlegel, H. B.; Scuseria, G. E.; Robb, M. A.; Cheeseman, J. R.; Scalmani, G.; Barone, V.; Mennucci, B.; Petersson, G. A.; Nakatsuji, H.; Caricato, M.; Li, X.; Hratchian, H. P.; Izmaylov, A. F.; Bloino, J.; Zheng, G.; Sonnenb, **2013**.

[73] A. D. Becke, *J. Chem. Phys.* **1988**, *38*, 3098–3100.

[74] A. D. Becke, *J. Chem. Phys.* **1993**, *98*, 5648–5652.

[75] S. Grimme, S. Ehrlich, L. Goerick, *J. Comput. Chem.* **2011**, *32*, 1456–1465.

[76] S. Grimme, J. Antony, S. Ehrlich, H. Krieg, *J. Chem. Phys.* **2010**, *132*, DOI 10.1063/1.3382344.

[77] P. J. Hay, W. R. Wadt, *J. Chem. Phys.* **1985**, *82*, 299–310.

[78] L. E. Roy, P. J. Hay, R. L. Martin, *J. Chem. Theory Comput.* **2008**, *4*, 1029–1031.

[79] F. Weigend, R. Ahlrichs, F. K. Gmbh, *Phys. Chem. Chem. Phys.* **2005**, *7*, 3297–3305.

[80] R. Ditchfield, W. J. Hehre, J. A. Pople, *J. Chem. Phys.* **1971**, *54*, 720–723.

[81] W. J. Hehre, K. Ditchfield, J. A. Pople, *J. Chem. Phys.* **1972**, *56*, 2257–2261.

[82] P. C. Hariharan, J. A. Pople, *Theor. Chim. Acta* **1973**, *28*, 213–222.

[83] M. M. Francl, W. J. Pietro, W. J. Hehre, J. S. Binkley, M. S. Gordon, D. J. DeFrees, J. A. Pople, *J. Chem. Phys.* **1982**, *77*, 3654–3665.

[84] M. S. Gordon, S. J. Binkley, J. A. Pople, W. J. Pietro, W. J. Hehre, **1982**, *104*, 2797–2803.